Osteoarthritis and Cartilage 26 (2018) 1691–1698

Osteoarthritis and Cartilage

Juvenile osteochondritis dissecans of the knee is a result of failure of the blood supply to growth cartilage and osteochondrosis☆

K. Olstad † *, K.G. Shea ‡, P.C. Cannamela ‡, J.D. Polousky §, S. Ekman ‖, B. Ytrehus ¶, C.S. Carlson #

† Department of Companion Animal Clinical Sciences, Equine Section, Norwegian University of Life Sciences, Oslo, Norway
‡ Department of Orthopedics, St. Luke's Sports Medicine, Boise, ID, USA
§ Children's Health Specialty Center Plano Campus, Andrews Institute/Children's Health, Plano, TX, USA
‖ Department of Biomedicine and Veterinary Public Health, Division of Pathology, Swedish University of Life Sciences, Uppsala, Sweden
¶ Terrestrial Department, Norwegian Institute for Nature Research, Trondheim, Norway
# Department of Veterinary Population Medicine, College of Veterinary Medicine, University of Minnesota, St. Paul, Minnesota, USA

ARTICLE INFO

Article history:
Received 9 October 2017
Accepted 9 June 2018

Keywords:
Osteochondrosis
Cartilage canal blood supply
Computed tomography
Histology
Ischemic chondronecrosis
Juvenile osteochondritis dissecans

SUMMARY

Objective: Juvenile osteochondritis dissecans (JOCD) is similar to osteochondrosis dissecans (OCD) in animals, which is the result of failure of the cartilage canal blood supply, ischemic chondronecrosis and delayed ossification, or osteochondrosis. The aim of the current study was to determine if osteochondrosis lesions occur at predilection sites for JOCD in children.

Method: Computed tomographic (CT) scans of 23 knees (13 right, 10 left) from 13 children (9 male, 4 female; 1 month to 11 years old) were evaluated for lesions consisting of focal, sharply demarcated, uniformly hypodense defects in the ossification front. Histological validation was performed in 11 lesions from eight femurs.

Results: Thirty-two lesions consisting of focal, uniformly hypodense defects in the ossification front were identified in the CT scans of 14 human femurs (7 left, 7 right; male, 7–11 years old). Defects corresponded to areas of ischemic chondronecrosis in sections from all 11 histologically validated lesions. Intra-cartilaginous secondary responses comprising proliferation of adjacent chondrocytes and vessels were detected in six and two lesions, whereas intra-osseous responses including accumulation of chondroclasts and formation of granulation tissue occurred in 10 and six lesions, respectively. One CT cyst-like lesion contained both a pseudocyst and a true cyst in histological sections.

Conclusion: Changes identical to osteochondrosis in animals were detected at predilection sites for JOCD in children, and confirmed to represent failure of the cartilage canal blood supply and ischemic chondronecrosis in histological sections.

Introduction

The term «osteochondritis dissecans» (OCD) was coined by König in 1887 to describe fragments that arise in joints with minimal or no history of trauma[1]. In humans, both adult and juvenile-onset OCD (JOCD) are recognized[2], whereas in animals onset is always in skeletally immature individuals[3]. In animals, it has been possible to examine developing OCD lesions and the earliest detectable changes occur within growth cartilage. In the present study the growth plate cartilage located between the primary and secondary centers of ossification (synonym: ossific nucleus) will be referred to as the physis (synonyms: metaphyseal growth plate,

☆ **Dedication:** The authors dedicate this manuscript to the memory of Professor Sten-Erik Olsson, DVM MD (1921–2000) and Associate Professor Sven Reiland, DVM (1935–2016), who were the first to suggest that osteochondritis dissecans was the same disease in humans and animals.

* Address correspondence and reprint requests to: K. Olstad, Norwegian University of Life Sciences, Faculty of Veterinary Medicine, Department of Companion Animal Clinical Sciences, Equine Section, Ullevålsveien 72, 0454, Oslo, Norway.
E-mail addresses: kristin.olstad@nmbu.no (K. Olstad), kevingshea@gmail.com (K.G. Shea), pcannamela@sandiego.edu (P.C. Cannamela), johnpolousky@childrens.com (J.D. Polousky), stina.ekman@slu.se (S. Ekman), bjornar.ytrehus@nina.no (B. Ytrehus), carls099@umn.edu (C.S. Carlson).

https://doi.org/10.1016/j.joca.2018.06.019

epiphyseal plate) [Fig. 1], and the growth cartilage between the secondary center of ossification and the articular cartilage as the epiphyseal growth cartilage [Fig. 1]. In contrast to articular cartilage, all growth cartilage has a temporary blood supply that runs within cartilage canals[4,5] [Fig. 1]. In epiphyseal growth cartilage, the blood supply is organized as anatomical end arteries that course into and out of the cartilage through the same canal[4,5]. As the individual matures, the blood supply gradually regresses by canals becoming filled with cartilage, known as chondrification, or by becoming incorporated into the advancing ossification front[5,6]. The mid-portion of the canal is incorporated prior to the proximal and distal portions, and recent studies in piglets and foals indicate that the blood supply sometimes fails during this process, resulting in ischemic necrosis of chondrocytes around the distal canal portion[5,6]. Only chondrocytes at intermediate depth of growth cartilage are susceptible to ischemia[4,7]. As the ossification front advances, the area of ischemic chondronecrosis resists replacement by bone and causes a focal delay in endochondral ossification[7]. By 1978, identical areas of disturbed ossification had been identified at OCD predilection sites in six animal species, and Olsson & Reiland proposed that they should be called “osteochondrosis”[3]. Cross-sectional studies indicated that osteochondrosis could progress to spontaneous resolution, pseudo- or true subchondral bone cysts, or pathologic OCD fracture[3,8,9]. Subsequently, the pathogenesis was reproduced by transecting the growth cartilage blood supply surgically in piglets[4,10], foals[7] and goats[11].

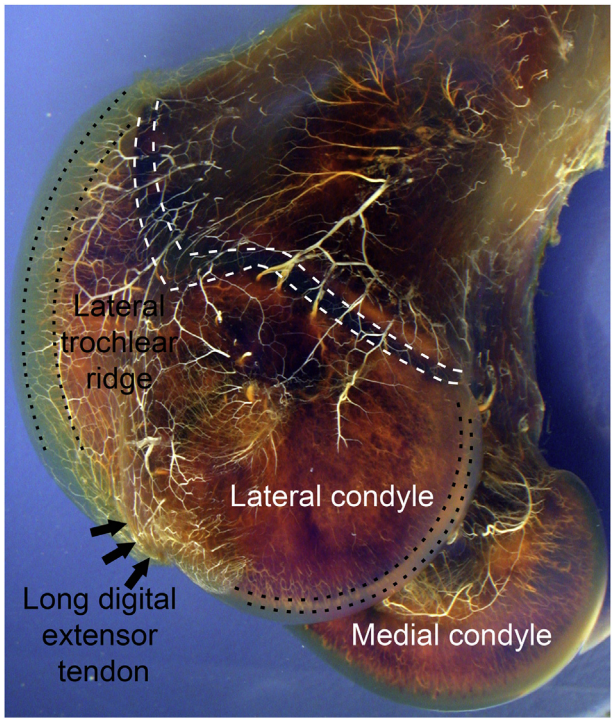

Fig. 1. Terminology used. Femur from a 4-week-old foal. The arterial side of the circulation is perfused with barium, and the soft tissues are rendered translucent by the modified Spalteholz method. Mineralized bone is visible as purple/orange-colored tissue deep to translucent soft tissue. The growth plate cartilage (between white stippled lines) located between the primary and secondary centers of ossification will be referred to as the physis (synonyms: metaphyseal growth plate, epiphyseal plate). The growth cartilage between the secondary center of ossification and the articular cartilage will be referred to as the epiphyseal growth cartilage (between black dotted lines). The secondary center of ossification (between the white stippled lines and black dotted lines) is also known as the ossific nucleus. Arrows: origin of the long digital extensor tendon, which carries blood vessels that enter cartilage.

The clinical features of animal OCD are highly similar to JOCD[8,9,12], thus, there is reason to believe that JOCD may also be a result of osteochondrosis. Ideally, predilection sites should be examined histologically but the only specimens that tend to be available in children are from chronic lesions poorly suited for studying lesion development[13]. Recently, the results of histological animal studies were translated to advanced diagnostic imaging. Vascular failure was initially detected using *ex vivo* arterial contrast-enhanced micro-computed tomography[14], and osteochondrosis was later monitored *in vivo* using non-contrast conventional computed tomography (CT)[15]. Vascular failure, ischemic chondronecrosis and osteochondrosis have since been monitored in animals using magnetic resonance imaging (MRI)[11,16,17]. Imaging requires validation and for the first time, the authors were privileged to gain access to entire femurs from young children that had been imaged using CT[18,19] and were available for histology.

The aim of the current study was to determine if vascular failure, ischemic chondronecrosis and osteochondrosis occur at predilection sites for JOCD in children.

Method

Study sample

The study sample represented re-examination of 23 knees from 13 children 1 month to 11 years old previously CT-scanned for ligament attachments using metal markers[18,19]. Children were assigned ascending numbers by age, then degree of CT ossification (Table I). The specimens came from an allograft facility that had received family consent for use of tissue for research (www.allosource.com). The study was approved by the Norwegian Regional Ethical Committee (Ref. no: 2017/2536). The review boards of all participating institutions were consulted and review deemed unnecessary for cadaver study.

Computed tomography

Knees were scanned in a 16-slice helical CT scanner (GE LightSpeed 16, GE Healthcare, Cincinnati, Ohio, USA). Scans were acquired in a transverse plane using a slice thickness of $\leq$2 mm.

Scans were evaluated by a veterinary radiologist with 18 years' experience and 71.5 % agreement[15]. Evaluation was blinded with respect to specimen identity. Each femur was evaluated in three orthogonal planes and as volume-rendered models. The bone contour, representing the ossification front, was inspected. Irregularities that were peripheral, gradual and diffuse were deemed within normal limits for growing bone. Changes consisting of focal, sharply demarcated, uniformly hypodense defects in or near the ossification front were interpreted as lesions[20]. Defects had to be detectable in $\geq$1 slice in at least two planes to count as lesions. Defects at sites of nutrient artery entry (e.g., the intercondylar fossa) or synovial fossae (e.g., the trochlear groove) were disregarded. Osteochondrosis occurs bilaterally in >50 % of cases[21], and changes that met the criteria were therefore interpreted as lesions even if they were symmetrical.

Lesion location was recorded by femur and region, subdivided into the medial condyle, lateral condyle, lateral trochlear ridge and medial trochlear ridge. Geometry was noted in terms of whether lesions comprised single or multiple closely adjacent defects, referred to as lobes. Lesion size was reported subjectively as small, medium, large or extra-large. Secondary responses[9] were recorded. Responses in growth cartilage included proliferation of adjacent viable chondrocytes and blood vessels, with subsequent formation of reparative ossification centers around proliferating vessels; only the latter is detectable in non-contrast CT scans as mineralized

Table I
Study sample and distribution of lesions per child

Child no.	Age	Sex	Limb	Diagnosis	Medial condyle	Lateral condyle	Lateral trochlear ridge	Lesions per femur	Lesions per child
1	1 month	Female	Right	Non-diagnostic scan	–	–	–	–	–
2	11 months	Male	Left	Non-diagnostic scan	–	–	–	–	–
			Right	Non-diagnostic scan	–	–	–	–	–
3	7 years	Male	Left	Lesions	1[A]	1[B]	0	2	5
			Right	Lesions	1	1[C]	1	3	
4	7 years	Female	Left	Normal	0	0	0	0	0
			Right	Normal	0	0	0	0	
5	8 years	Male	Left	Lesions	1[D]	0	1[E]	2	4
			Right	Lesions	1	0	1[F]	2	
6	8 years	Male	Left	Lesions	1	1	1[G]	3	6
			Right	Lesions	1	1	1	3	
7	8 years	Male	Right	Lesions	1	1	0	2	2
8	10 years	Male	Left	Lesion	1	0	0	1	1
			Right	Normal	0	0	0	0	
9	10 years	Female	Left	Normal	0	0	0	0	0
			Right	Normal	0	0	0	0	
10	10 years	Female	Right	Normal	0	0	0	0	0
11	11 years	Male	Left	Lesions	1	1[H]	1	3	5
			Right	Lesions	1	1	0	2	
12	11 years	Male	Left	Lesions	1	0	1	2	4
			Right	Lesions	1	0	1	2	
13	11 years	Male	Left	Lesions	1[I]	1[J]	0	2	5
			Right	Lesions	1[K]	1	1	3	
Sum					14 (44 %)	9 (28 %)	9 (28 %)	32	32
Range								0–3	0–6
Median								2	2

[A–K]Lesions processed for histological validation.

bodies superficial to lesions[20]. Responses in bone included chondroclast recruitment and formation of fibro-vascular granulation tissue capable of undergoing intramembranous ossification, detectable as marginal sclerosis[20]. Continued ossification around lesions was noted, including whether this resulted in a cyst-like appearance[22].

Histology

Funding permitted processing of 11 lesions for histology, originating from eight femurs of five children. The 11 lesions were assigned ascending capital letters by child, followed by location (Table I). Eight of the 11 lesions were chosen because they were among the largest in CT scans, and likely to be visible on a cut surface. The remaining three lesions were chosen because they occurred in individuals already selected for validation and were detectable without serial sectioning.

The eight femurs were sawed into 3–5 mm thick slabs in the parasagittal plane for trochlear ridge lesions and the frontal plane for condylar lesions. Slabs were fixed in 4% phosphate-buffered formaldehyde and decalcified in 10% ethylenediaminetetraacetic acid. Smaller blocks were cut from the slabs to fit into cassettes measuring 32 × 25 × 5 mm, guided by macroscopically visible focal irregularity of the ossification front, or by the CT scans. The blocks were paraffin-embedded, sectioned and stained with hematoxylin and eosin.

Histological sections were evaluated by a panel of three professors of veterinary pathology with a collective 90 years' experience. The three observers agreed on all final diagnoses. Criteria for evaluation were identical to previous animal studies[20,22], but briefly: necrotic cartilage canals were defined by necrosis and lysis of endothelial and mesenchymal cells[4]. Coagulative necrosis of chondrocytes was defined by pyknosis or karyolysis, cellular shrinkage, cytoplasmic eosinophilia and focally altered matrix staining[23]. Pseudocysts were defined by areas of ischemic chondronecrosis surrounded by, but not separated from bone by any distinct lining, whereas true cysts were defined as dilated structures lined by fibrous tissue and located within areas of ischemic chondronecrosis[22].

Results

Study sample

Three CT scans from two children were non-diagnostic because a combination of small secondary ossification center and large metal markers[18,19] meant there was no ossification front to inspect. Six femurs from four children (3 female, 1 male with contralateral lesion) were normal and 14 femurs from eight children (male, 7–11 years old) contained lesions (Table I). The 14 affected femurs contained 32 lesions, the distribution of which is shown in Table I.

Computed tomography

The results of CT evaluation are summarized in Table II.

All lesions contained one or more uniformly hypodense defects in the ossification front and three different shapes were observed. In 4/32 lesions, there was a single lobe that was triangular or round/ovoid in 2D slice images [Fig. 2(A)] and conical or hemi-spherical in 3D volume-rendered models. Twelve of 32 lesions were multilobulated, and adjacent lobes were shifted with respect to each other and could therefore be described as “stair-step” lesions [Fig. 2(B)]. In the remaining 6/32 lesions, the defect was linear in 2D and sheet-like in 3D models [Fig. 2(C) and (D)], and represented a particular stage of repair described below.

Nine of the 32 lesions (Table II) contained a focal area of bone hyperdensity, or mineralized body within the cartilage superficial to the primary hypodense defect [Fig. 2(C–E)], compatible with separate centers of reparative endochondral ossification. In three lesions, the ossification centers were completely separated from the lateral trochlear ridge by the sheet-like defects described above [Fig. 2(C) and (D)]. In two lesions, the centers were connected to the medial condyle by a thin, mineralized pedicle [Fig. 2(E)] and in the

Table II
Computed tomographic evaluation per lesion

Child no.	Limb	Femur region	Defect shape	Size	Mineralized body	Sclerosis	Continued ossification	Histological lesion no.
3	Left	MC*	Multi-lobe	M§	–	Speck or partial rim	–	A
	Left	LC†	Single lobe	M/L‖	–	–	Marked and cyst-like	B
	Right	MC	Multi-lobe	S¶	–	Extensive or complete rim	–	–
	Right	LC	Multi-lobe	S/M	–	Speck or partial rim	–	C
	Right	LTR‡	Linear	S	Bone bridging	–	–	–
5	Left	MC	Multi-lobe	M/L	–	Extensive or complete rim	–	D
	Left	LTR	Single lobe	S	Bone bridging	–	–	E
	Right	MC	Multi-lobe	S	–	–	Marked	–
	Right	LTR	Linear	XL#	Completely separate	–	–	F
6	Left	MC	Single lobe	S	–	Speck or partial rim	–	–
	Left	LC	Single lobe	S	–	–	Marked	–
	Left	LTR	Linear	M	Bone bridging	–	–	G
	Right	MC	Single lobe	S	–	Extensive or complete rim	–	–
	Right	LC	Single lobe	S	–	Extensive or complete rim	–	–
	Right	LTR	Linear	S	Bone bridging	–	–	–
7	Right	MC	Multi-lobe	S	–	–	Moderate	–
	Right	LC	Single lobe	L	–	–	Marked and cyst-like	–
8	Left	MC	Multi-lobe	S	–	–	Marked	–
11	Left	MC	Multi-lobe	S	–	Extensive or complete rim	–	–
	Left	LC	Single lobe	M/L	–	–	Marked and cyst-like	H
	Left	LTR	Single lobe	S	–	–	Marked and cyst-like	–
	Right	MC	Single lobe	S	–	Extensive or complete rim	–	–
	Right	LC	Single lobe	S	–	Extensive or complete rim	–	–
12	Left	MC	Multi-lobe	L	Connected by a stalk	–	–	–
	Left	LTR	Linear	S	Completely separate	–	–	–
	Right	MC	Multi-lobe	L	Connected by a stalk	–	–	–
	Right	LTR	Linear	S	Completely separate	–	–	–
13	Left	MC	Multi-lobe	L	–	–	Moderate	I
	Left	LC	Single lobe	L	–	Speck or partial rim	–	J
	Right	MC	Multi-lobe	S/M	–	Speck or partial rim	–	K
	Right	LC	Single lobe	S	–	–	–	–
	Right	LTR	Single lobe	S	–	–	–	–

* MC: medial condyle.
† LC: lateral condyle.
‡ LTR: lateral trochlear ridge.
§ M: medium.
‖ L: large.
¶ S: small.
# XL: extra-large.

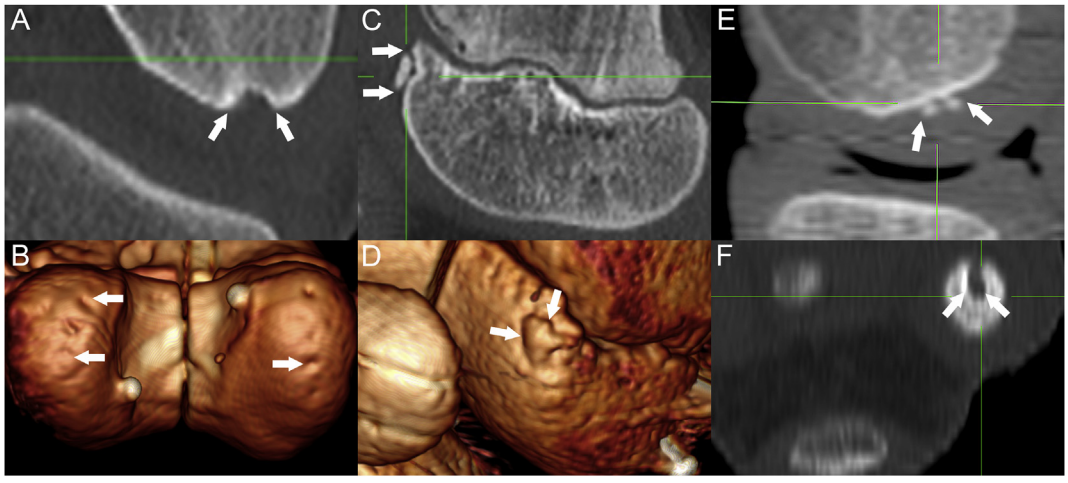

Fig. 2. Computed tomographic observations. (A) Child 3, 7-year-old male, left femur, frontal slice: there is a triangular single lobe defect (between arrows) in the lateral condyle. (B) Child 7, 8-year-old male, right femur, posterior view of volume-rendered model: there is a single lobe defect in the lateral condyle (arrow) and multi-lobulated, proximo-distally staggered "stair-step" defect in the medial condyle (between arrows). (C) Child 5, 8-year-old male, right femur, parasagittal slice: there is a linear hypodense defect and mineralized body (between arrows), representing a separate center of reparative endochondral ossification, at the lateral trochlear ridge. (D) Anterior-lateral-proximal oblique view of volume-rendered model of the lesion in Fig. 2(C): the linear defect was sheet-like and the ossification center (between arrows) roughly spherical in 3D. (E) Child 12, 11-year-old male, left femur: there are two mineralized bodies (between arrows) connected to the medial condyle by a thin, mineralized pedicle or stalk. (F) Transverse slice from the lesion in Fig. 2(A): ossification has progressed so far that the primary hypodense defect (between arrows) is almost completely surrounded by bone, characterized as a cyst-like appearance.

remaining four lesions, there was a variable amount of bone bridging.

In 12/32 lesions, hyperdense or sclerotic areas were detected in the bone immediately subjacent to primary ossification front defects (Table II). The sclerosis was partial in 5/12 lesions and formed an extensive or complete rim in 7/12 lesions.

Nine of the 32 lesions were located deeper and surrounded by more bone than the others, representing continued endochondral ossification adjacent to lesions (Table II). In three lateral condylar lesions and one lateral trochlear lesion, ossification had progressed so far that the hypodense defect was almost completely surrounded by bone in individual CT slices, characterized as cyst-like lesions [Fig. 2(F)].

Histology

The results of histological validation are summarized in Table III.

Primary hypodense defects in CT scans corresponded to areas of necrotic epiphyseal growth cartilage in or immediately deep to the ossification front in sections from all 11 lesions [Fig. 3(A)]. The necrotic cartilage was centered on necrotic cartilage canals [Fig. 3((A), (B), (C): normal comparison)]. Together, these observations supported the conclusion that hypodense defects were due to ischemic chondronecrosis. All chondrocytes around necrotic cartilage canals lacked nuclei, i.e., were necrotic. Due to delayed fixation, chondrocytes distant from necrotic canals often also lacked nuclei. It was, however, still possible to identify the superficial boundary of the ischemic chondronecrosis based on cellular shrinkage and altered matrix staining.

Intra-cartilaginous secondary responses were observed superficially and laterally adjacent to lesions, comprising modest proliferation of adjacent chondrocytes and vessels detected in sections from six and two lesions, respectively (Table III). The mineralized bodies in lesions E and F (Table II) were captured in sections, where they corresponded to osteoid-producing osteoblasts on the margins of cartilage canals containing proliferating vessels, i.e., separate centers of reparative endochondral ossification [Fig. 3(D)]. The sheet-like defects separating the ossification centers from the femur consisted of areas of ischemic chondronecrosis [Fig. 3(D)].

Intra-osseous secondary responses occurred within the bone deep to lesions, including accumulation of multi-nucleated giant cells on the margin of 10 lesions (Table III), interpreted as chondroclasts engaged in phagocytosis of the necrotic cartilage. Fibrovascular granulation tissue was present and showed evidence of intra-membranous ossification towards the interface with bone deep to six lesions. The ossification in lesions B, E, F and I had produced insufficient bone for detectable sclerosis, whereas in lesions C and J, intra-membranous ossification in sections corresponded to partial sclerotic rims in CT scans (Table II). The incomplete sclerotic rims in lesions A and D were not captured in sections.

In eight lesions, there were areas of ischemic chondronecrosis completely surrounded by bone on all sides that were therefore characterized as pseudocysts in histological sections (Table III). In seven of these lesions, multi-planar reconstruction confirmed that the appearance was a sectioning angle artefact not resulting in any cyst-like appearance in CT scans. The eighth lesion B that resulted in a cyst-like appearance in CT scans contained both a pseudocyst [Fig. 3(E)] and dilated remnants of necrotic vessels, i.e., true cysts [Fig. 3(F)].

Discussion

Changes identical to osteochondrosis in animals were detected at predilection sites for JOCD in children.

The observed CT changes agree with previous imaging studies in children (multi-lobulated defects: spiculated pattern, reparative ossification centers: extra ossification centers, continued ossification/sheet-like defects: puzzle pieces[24–26]). The difference is that in children, these changes tend to be interpreted as normal variants[24–26], whereas in animals, they are interpreted as osteochondrosis[14,20]. The ossification front is normally irregular during growth. Several of the criteria used for differentiating normal from disease cannot be used in osteochondrosis, including lesion symmetry[21] and lack of symptoms[12]. The ages suggested by Jans *et al.*[25,26] for separating variants from disease mirror the development pattern of osteochondrosis in horses of resolving or progressing to OCD before specific age thresholds[27]. Bone marrow edema is often considered a disease marker[24,25], but represents interpretation of a fluid signal in MRI scans that lack the spatio-temporal resolution to distinguish static interstitial edema from dynamic capillary flow in granulation tissue (discussed further, below). The criterion for differentiating between normal and disease in animals is whether the irregularity contains histopathological changes. When translated on a histology-section-to-CT-slice basis, an easily recognizable pattern emerged of normal variants being diffuse, gradual and peripheral and osteochondrosis defects being focal and sharply demarcated at OCD predilection sites[14,20]. Clearly, there is a call for publishing more on animal-validated identification of normal CT variants in human journals. The definitive disease criteria in animals are identifiable by non-invasive imaging techniques, meaning that ossification irregularities in children could be studied using protocols capable of identifying vascular failure, chondronecrosis and/or associated matrix change[11,16,17,28], to make differentiation more definitive in humans.

Table III
Histological validation per lesion

Lesion no.	Cartilage canal and chondrocyte necrosis	Adjacent chondrocyte proliferation	Adjacent vessel proliferation	Reparative endochondral ossification center	Chondroclast recruitment	Fibro-vascular granulation tissue	Intra-membranous ossification	Pseudocyst	True cyst
A	+	−	−	−	+	−	−	−	−
B	+	+	+	−	+	+	+	+	+
C	+	+	−	−	+	+	+	+	−
D	+	−	−	−	+	−	−	+	−
E	+	−	+	+	+	+	+	+	−
F	+	+	−	+	+	+	+	+	−
G	+	−	−	−	−	−	−	+	−
H	+	−	−	−	+	−	−	−	−
I	+	+	−	−	+	+	+	−	−
J	+	+	−	−	+	+	+	+	−
K	+	+	−	−	+	−	−	+	−

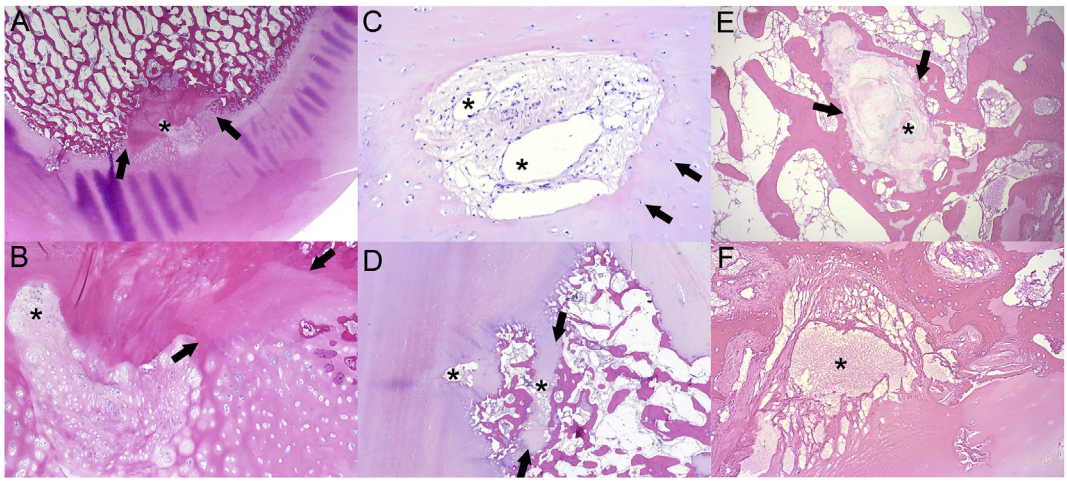

Fig. 3. Histological validation. (A) Lesion B from child 3, 7-year-old male, left femur, lateral condyle, also shown in Fig. 2(A), frontal section: the hypodense defect in Fig. 2(A) corresponds to an area of necrotic epiphyseal growth cartilage (between arrows), centered on a necrotic cartilage canal (asterisk), i.e., an area of ischemic chondronecrosis within the ossification front. (B) Higher power magnification of lesion B. The asterisk is in the same position within the necrotic cartilage canal as in Fig. 3(A). There is an area of coagulative chondrocyte necrosis within the ossification front (between arrows). (C) Normal comparison from child 6, 8-year-old male, left femur, lateral trochlear ridge. There is a cartilage canal with venous luminae (asterisks), surrounded by morphologically viable, nucleated chondrocytes (arrows). (D) Lesion F, child 5, 8-year-old male, left femur, lateral trochlear ridge, also shown in Fig. 2(C), parasaggital section: there is an area of chondrocyte necrosis (between arrows), centered on necrotic cartilage canals (asterisks) that corresponds to the linear hypodense defect in Fig. 2(C). Superficial to this, there are osteoid-producing osteoblasts, i.e., a separate center of reparative endochondral ossification corresponding to the mineralized body in Fig. 2(C). (E) The cyst-like portion of lesion B also shown in Fig. 2(F) contains a solid area of ischemic chondronecrosis (between arrows; asterisk: necrotic cartilage canal) completely surrounded by bone, i.e., a pseudocyst. (F) Lesion B contains a dilated remnant of a necrotic vessel (asterisk), i.e., a true cyst.

In the current specimens, focal defects in CT scans corresponded to vascular failure and ischemic chondronecrosis. For decades, it has been debated whether J/OCD is the result of primary disease of cartilage or bone. Veterinarians first considered that vascular failure was the result of micro-fractures at the ossification front[6]. Cartilage canal vascular failure can also occur secondary to bacteremia, documented in chickens[29], pigs[30] and foals[31]. However, when examined by micro-CT with the power to detect them, micro-fractures were not present in genuinely early lesions of osteochondrosis[14]. Likewise, bacteremia could only be the cause of a minority of lesions. The majority of cartilage canal vascular failure in animals therefore occurs without evidence of preceding or concurrent primary disease of bone. The only primary disease that has been identified is failure of the cartilage canal blood supply, and when osteochondrosis is surgically induced, it is through interventions to epiphyseal growth cartilage alone, avoiding subchondral bone[4,7,10,11]. It is therefore certain that osteochondrosis in animals is the result of primary disease of the cartilage canal blood supply. The suggestion that JOCD is due to primary bone disease is the logical result of examining chronic lesions[13], around which ossification has had time to advance. To study developing lesions, children must be examined before symptoms debut, i.e., before 6 years of age[32,33]. The current results make it likely that JOCD is a result of primary disease of the cartilage canal blood supply in children also.

Osteochondrosis can be monitored longitudinally[15], and animal studies point to factors that influence progression. Lesion size was a strong prognostic variable in human studies[34,35]. However, size alone does not fully explain progression in humans[34,35] or animals[36], and secondary responses may be more important than previously thought. Ribbing[37] hypothesized that extra ossification centers in humans were particularly susceptible to fracture. This is corroborated by animal studies where the cartilage separating ossification centers from the underlying bone is necrotic[7,14], and therefore has weakened extra-cellular matrix[38]. The OCD lesion in one experimental foal occurred through the area of necrosis before notable bone bridging was present[7]. It is possible that restriction of activity whilst bone bridges form can avert progression to pathologic fracture in some cases[34,35,39,40].

Lesions in animals contain three components: ischemic chondronecrosis, fibro-vascular granulation tissue and dilated vessels/true cysts[22,36]. It may become necessary to quantify the relative proportions of these components in order to predict progression. The volume of chondronecrosis is important because it must be removed by phagocytosis (or debridement) for resolution to occur[14]. In human studies, granulation tissue is assigned positive[41] or negative[42] roles. Animal studies confirm both, as granulation tissue contains chondroclasts for removal of chondronecrosis and stem cells[23,36]. Cysts were, however, more commonly present within granulation tissue than within areas of chondronecrosis[22], and cysts were associated with poorer prognosis in both humans[34,43] and animals[22]. In foals, true cysts were associated with mechanisms that led to progressive enlargement of the cavity and cavities above a certain size were associated with infolding of the overlying cartilage and OCD[22]. One of the most important goals in JOCD is to determine lesion stability[2,33,44]. Prediction of stability has partly been based on identification of a high fluid signal line deep to lesions in T2-weighted MRI, but the technique has limited accuracy[41,43]. Animal studies support that the high signal should be interpreted as fluid within granulation tissue capillaries[41,42], rather than edema. This potentially explains how lesions can be either stable or unstable deep to intact articular cartilage. Lesions consisting of solid chondronecrosis are likely to be stable[22], whereas lesions containing softer granulation tissue may be stable or unstable depending on the volume of granulation tissue[23,36], and lesions containing large cysts are likely to be unstable due to the previous association with cartilage infolding[22]. Determining the relative proportions of chondronecrosis, granulation tissue and cysts within lesions may therefore be important for understanding lesion stability, as well as for predicting progression.

Finally, biomechanical force is probably the single-most important factor influencing progression of osteochondrosis to J/OCD[2,8,9,32,33]. It is necessary to subdivide epiphyses into load-bearing, impingement and traction regions[45]. Outcome is a result

of the balance between lesions arising and resolving[15,27] and in piglet knees, lesions arose bi-axially, but the proportion that resolved was higher in lateral than medial regions[15]. Medial sites experience greater load than lateral sites and in older pigs, OCD is more common in the medial than the lateral condyle[46]. This is also the likely explanation for the fact that current early defects were identified in 7.5/10 of children (Table I); much higher than the reported incidence of JOCD[32,33]. Progression to J/OCD at the medial condyle has been associated with impingement from the tibial spine[2,32,44,47]. The posterior cruciate ligament attaches in this region[48], making it a traction site also, and ligament traction can feasibly influence initiation [Fig. 1], response to[49,50] and avulsion of ischemic lesions[36], i.e., modify most aspects of pathogenesis. Thus, variants of a progression model are required to account for different factors acting at load-bearing, impingement and traction epiphyseal regions.

Changes identical to osteochondrosis in animals were detected at predilection sites for JOCD in children, and confirmed to represent failure of the cartilage canal blood supply and ischemic chondronecrosis by histology. Further validation is required, but comparison to the documented progression in animals provides strong evidence that ischemic chondronecrosis in children can progress to JOCD. These results suggest that JOCD is the outcome of a disease process that starts at a much younger age than previously thought.

Author contributions

All authors contributed substantially to all aspects of the study. KO performed data acquisition and analysis, and drafted the manuscript. KGS, PCC and JDP performed data collection and revised the manuscript critically. SE, BY and CSC performed data analysis and revised the manuscript critically. All authors gave final approval of the submitted version of the manuscript. KO (kristin.olstad@nmbu.no) assumes responsibility for the integrity of the work as a whole.

Conflict of interest

None declared.

Role of the funding source

The manuscript had no specific funding source. The funding sources of the original human and animal studies had no role in the study design, collection, analysis, interpretation, writing of the manuscript or decision to submit the manuscript for publication.

Studies involving animals

Not applicable.

Acknowledgements

The authors are grateful to Tom Cycyota, Peter Armstrong, Todd Huft and Lisa Houck at Allosource, Centennial, Colorado, USA for their assistance in providing the human specimens. The authors also thank Eli Grindflek and Jørgen Kongsro at Norsvin, Hamar, Norway for support with the porcine and equine CT scans, and the staff at the University of Minnesota Masonic Cancer Center Comparative Pathology Shared Resource for preparation of the human histological sections.

References

1. Konig F. The classic: on loose bodies in the joint. 1887. Clin Orthop Relat Res 2013;471:1107–15.
2. Edmonds EW, Polousky J. A review of knowledge in osteochondritis dissecans: 123 years of minimal evolution from konig to the ROCK study group. Clin Orthop Relat Res 2012;471:1118–26.
3. Olsson SE, Reiland S. The nature of osteochondrosis in animals. Summary and conclusions with comparative aspects on osteochondritis dissecans in man. Acta Radiol Suppl 1978;358:299–306.
4. Carlson CS, Meuten DJ, Richardson DC. Ischemic necrosis of cartilage in spontaneous and experimental lesions of osteochondrosis. J Orthop Res 1991;9:317–29.
5. Olstad K, Ytrehus B, Ekman S, Carlson CS, Dolvik NI. Epiphyseal cartilage canal blood supply to the tarsus of foals and relationship to osteochondrosis. Equine Vet J 2008;40:30–9.
6. Ytrehus B, Ekman S, Carlson CS, Teige J, Reinholt FP. Focal changes in blood supply during normal epiphyseal growth are central in the pathogenesis of osteochondrosis in pigs. Bone 2004;35:1294–306.
7. Olstad K, Hendrickson EHS, Carlson CS, Ekman S, Dolvik NI. Transection of vessels in epiphyseal cartilage canals leads to osteochondrosis and osteochondrosis dissecans in the femoropatellar joint of foals; a potential model of juvenile osteochondritis dissecans. Osteoarthritis Cartilage 2013;21:730–8.
8. Ytrehus B, Carlson CS, Ekman S. Etiology and pathogenesis of osteochondrosis. Vet Pathol 2007;44:429–48.
9. Olstad K, Ekman S, Carlson CS. An update on the pathogenesis of osteochondrosis. Vet Pathol 2015;52:785–802.
10. Ytrehus B, Andreas Haga H, Mellum CN, Mathisen L, Carlson CS, Ekman S, *et al*. Experimental ischemia of porcine growth cartilage produces lesions of osteochondrosis. J Orthop Res 2004;22:1201–9.
11. Toth F, Nissi MJ, Wang L, Ellermann JM, Carlson CS. Surgical induction, histological evaluation, and MRI identification of cartilage necrosis in the distal femur in goats to model early lesions of osteochondrosis. Osteoarthritis Cartilage 2015;23:300–7.
12. McCoy AM, Toth F, Dolvik NI, Ekman S, Olstad K, Ytrehus B, *et al*. Articular osteochondrosis: a comparison of naturally-occurring human and animal disease. Osteoarthritis Cartilage 2013;21:1638–47.
13. Shea KG, Jacobs Jr JC, Carey JL, Anderson AF, Oxford JT. Osteochondritis dissecans knee histology studies have variable findings and theories of etiology. Clin Orthop Relat Res 2013;471:1127–36.
14. Olstad K, Cnudde V, Masschaele B, Thomassen R, Dolvik NI. Micro-computed tomography of early lesions of osteochondrosis in the tarsus of foals. Bone 2008;43:574–83.
15. Olstad K, Kongsro J, Grindflek E, Dolvik NI. Consequences of the natural course of articular osteochondrosis in pigs for the suitability of computed tomography as a screening tool. BMC Vet Res 2014;10(1):212.
16. Wang L, Nissi MJ, Toth F, Johnson CP, Garwood M, Carlson CS, *et al*. Quantitative susceptibility mapping detects abnormalities in cartilage canals in a goat model of preclinical osteochondritis dissecans. Magn Reson Med 2017 Mar;77(3):1276–83.
17. Toth F, David FH, LaFond E, Wang L, Ellermann JM, Carlson CS. In vivo visualization using MRI T2 mapping of induced osteochondrosis and osteochondritis dissecans lesions in goats undergoing controlled exercise. J Orthop Res 2017 Apr;35(4):868–75.
18. Shea KG, Polousky JD, Jacobs Jr JC, Ganley TJ, Aoki SK, Grimm NL, *et al*. The relationship of the femoral physis and the medial patellofemoral ligament in children: a cadaveric study. J Pediatr Orthop 2014;34:808–13.
19. Shea KG, Styhl AC, Jacobs Jr JC, Ganley TJ, Milewski MD, Cannamela PC, *et al*. The relationship of the femoral physis and

the medial patellofemoral ligament in children: a cadaveric study. Am J Sports Med 2016;44:2833–7.
20. Olstad K, Kongsro J, Grindflek E, Dolvik NI. Ossification defects detected in CT scans represent early osteochondrosis in the distal femur of piglets. J Orthop Res 2014;32:1014–23.
21. Grøndahl AM, Dolvik NI. Heritability estimations of osteochondrosis in the tibiotarsal joint and of bony fragments in the palmar/plantar portion of the metacarpo- and metatarsophalangeal joints of horses. J Am Vet Med Assoc 1993;203:101–4.
22. Olstad K, Ostevik L, Carlson CS, Ekman S. Osteochondrosis can lead to formation of pseudocysts and true cysts in the subchondral bone of horses. Vet Pathol 2015;52:862–72.
23. Olstad K, Ytrehus B, Ekman S, Carlson CS, Dolvik NI. Early lesions of osteochondrosis in the distal tibia of foals. J Orthop Res 2007;25:1094–105.
24. Gebarski K, Hernandez RJ. Stage-I osteochondritis dissecans versus normal variants of ossification in the knee in children. Pediatr Radiol 2005;35:880–6.
25. Jans LB, Jaremko JL, Ditchfield M, Huysse WC, Verstraete KL. MRI differentiates femoral condylar ossification evolution from osteochondritis dissecans. A new sign. Eur Radiol 2011;21:1170–9.
26. Jans L, Jaremko J, Ditchfield M, De Coninck T, Huysse W, Moon A, *et al*. Ossification variants of the femoral condyles are not associated with osteochondritis dissecans. Eur J Radiol 2012;81:3384–9.
27. Dik KJ, Enzerink E, van Weeren PR. Radiographic development of osteochondral abnormalities in the hock and stifle of Dutch Warmblood foals, from age 1 to 11 months. Equine Vet J Suppl 1999;31:9–15.
28. Martel G, Crowley D, Olive J, Halley J, Laverty S. Ultrasonographic screening for subclinical osteochondrosis of the femoral trochlea in foals (28-166 days old): a prospective farm study. Equine Vet J 2018 May;50(3):312–20.
29. Speers DJ, Nade SM. Ultrastructural studies of adherence of Staphylococcus aureus in experimental acute hematogenous osteomyelitis. Infect Immun 1985;49:443–6.
30. Denecke R, Trautwein G, Kaup FJ. The role of cartilage canals in the pathogenesis of experimentally induced polyarthritis. Rheumatol Int 1986;6:239–43.
31. Wormstrand B, Østevik L, Ekman S, Olstad K. Septic arthritis/osteomyelitis may lead to osteochondrosis-like lesions in foals. Vet Pathol 2018, https://doi.org/10.1177/0300985818777786.
32. Grimm NL, Weiss JM, Kessler JI, Aoki SK. Osteochondritis dissecans of the knee: pathoanatomy, epidemiology, and diagnosis. Clin Sports Med 2014;33:181–8.
33. Nepple JJ, Milewski MD, Shea KG. Research in osteochondritis dissecans of the knee: 2016 update. J Knee Surg 2016;29:533–8.
34. Krause M, Hapfelmeier A, Moller M, Amling M, Bohndorf K, Meenen NM. Healing predictors of stable juvenile osteochondritis dissecans knee lesions after 6 and 12 months of nonoperative treatment. Am J Sports Med 2013;41:2384–91.
35. Wall EJ, Vourazeris J, Myer GD, Emery KH, Divine JG, Nick TG, *et al*. The healing potential of stable juvenile osteochondritis dissecans knee lesions. J Bone Joint Surg Am 2008;90:2655–64.
36. Olstad K, Ytrehus B, Carlson CS, Ekman S, Dolvik NI. Early lesions of articular osteochondrosis in the distal femur of foals. Vet Pathol 2011;48:1165–75.
37. Ribbing S. The hereditary multiple epiphyseal disturbance and its consequences for the aetiogenesis of local malacias–particularly the osteochondrosis dissecans. Acta Orthop Scand 1955;24:286–99.
38. Carlson CS, Hilley HD, Henrikson CK, Meuten DJ. The ultrastructure of osteochondrosis of the articular-epiphyseal cartilage complex in growing swine. Calcif Tissue Int 1986;38:44–51.
39. Takahara M, Shundo M, Kondo M, Suzuki K, Nambu T, Ogino T. Early detection of osteochondritis dissecans of the capitellum in young baseball players. Report of three cases. J Bone Joint Surg Am 1998;80:892–7.
40. Takahara M, Ogino T, Takagi M, Tsuchida H, Orui H, Nambu T. Natural progression of osteochondritis dissecans of the humeral capitellum: initial observations. Radiology 2000;216:207–12.
41. O'Connor MA, Palaniappan M, Khan N, Bruce CE. Osteochondritis dissecans of the knee in children. A comparison of MRI and arthroscopic findings. J Bone Joint Surg Br 2002;84:258–62.
42. Zbojniewicz AM, Stringer KF, Laor T, Wall EJ. Juvenile osteochondritis dissecans: correlation between histopathology and MRI. AJR Am J Roentgenol 2015;205:W114–23.
43. Zbojniewicz AM, Laor T. Imaging of osteochondritis dissecans. Clin Sports Med 2014;33:221–50.
44. Wall E, Von Stein D. Juvenile osteochondritis dissecans. Orthop Clin N Am 2003;34:341–53.
45. Goff CW. Legg-Calvé-Perthes syndrome and related osteochondroses of youth. Springfield, Illinois, USA: Charles C. Thomas; 1954.
46. Reiland S. Morphology of osteochondrosis and sequelae in pigs. Acta Radiol Suppl 1978;358:45–90.
47. Grøndalen T. Osteochondrosis and arthrosis in pigs. VII. Relationship to joint shape and exterior conformation. Acta Vet Scand Suppl 1974;46:1–32.
48. Ishikawa M, Adachi N, Yoshikawa M, Nakamae A, Nakasa T, Ikuta Y, *et al*. Unique anatomic feature of the posterior cruciate ligament in knees associated with osteochondritis dissecans. Orthop J Sports Med 2016;4. 2325967116648138.
49. Trueta J. The normal vascular anatomy of the human femoral head during growth. J Bone Joint Surg Br 1957;39-B:358–94.
50. Olstad K, Ytrehus B, Ekman S, Carlson CS, Dolvik NI. Epiphyseal cartilage canal blood supply to the distal femur of foals. Equine Vet J 2008;40:433–9.